HHS Public Access

Author manuscript

Prostate. Author manuscript; available in PMC 2017 July 17.

Published in final edited form as:

Prostate. 2013 July ; 73(10): 1123–1133. doi:10.1002/pros.22662.

Obesity-Induced Diabetes and Lower Urinary Tract Fibrosis Promote Urinary Voiding Dysfunction in a Mouse Model

Mehrnaz Gharaee-Kermani[1], **Jose A. Rodriguez-Nieves**[1,2], **Rohit Mehra**[3], **Chad A. Vezina**[4], **Aruna V. Sarma**[1], and **Jill A. Macoska**[1,2,*]

[1]The Department of Urology, The University of Michigan, Ann Arbor, Michigan

[2]The Graduate Program in Cellular and Molecular Biology, The University of Michigan, Ann Arbor, Michigan

[3]The Department of Pathology, The University of Michigan, Ann Arbor, Michigan

[4]The Department of Comparative Biosciences, The University of Wisconsin, Madison, Wisconsin

Abstract

BACKGROUND—Progressive aging- and inflammation-associated fibrosis effectively remodels the extracellular matrix (ECM) to increase prostate tissue stiffness and reduce urethral flexibility, resulting in urinary flow obstruction and lower urinary tract symptoms (LUTS). In the current study, we sought to test whether senescence-accelerated mouse prone (SAMP)6 mice, which were reported to develop prostatic fibrosis, would also develop LUTS, and whether these symptoms would be exacerbated by diet-induced obesity and concurrent Type 2 Diabetes Mellitus (T2DM).

METHODS—To accomplish this, SAMP6 and AKR/J background strain mice were fed regular mouse chow, low fat diet chow, or high fat diet chow for 8 months, then subjected to glucose tolerance tests, assessed for plasma insulin levels, evaluated for urinary voiding function, and assessed for lower urinary tract fibrosis.

RESULTS—The results of these studies show that SAMP6 mice and AKR/J background strain mice develop diet-induced obesity and T2DM concurrent with urinary voiding dysfunction. Moreover, urinary voiding dysfunction was more severe in SAMP6 than AKR/J mice and was associated with pronounced prostatic and urethral tissue fibrosis.

CONCLUSIONS—Taken together, these studies suggest that obesity, T2DM, lower urinary tract fibrosis, and urinary voiding dysfunction are inextricably and biologically linked. Prostate.

Keywords

diet; bladder; prostate; fat; collagen

*Correspondence to: Jill A. Macoska, PhD, Department of Urology, The University of Michigan, 6217 Cancer Center, 1500 East Medical Center Drive, Ann Arbor, MI 48109-0944. jcoska@umich.edu.

INTRODUCTION

Benign prostatic hyperplasia (BPH) is one of the most common benign proliferative conditions associated with aging in men. BPH is a chronic, progressive disease of the prostate which conservatively affects 30–35% of men aged 60 or older and results in a significantly negative impact on quality of life [1–3]. This negative impact is due to various co-morbidities that develop concurrently with BPH that collectively produce lower urinary tract symptoms (LUTS) characteristic of lower urinary tract dysfunction, or LUTD. LUTD is itself a progressive disorder that is manifesting as urgency, nocturia, urinary frequency, weak urinary stream, and incomplete bladder emptying. Without effective treatment, LUTD can lead to bladder outlet obstruction (BOO) and subsequent bladder wall hypertrophy, increased bladder mass, and bladder dysfunction manifest as acute urinary retention, recurrent urinary tract infections, bladder stones, and, eventually, renal dysfunction [4]. Type 2 Diabetes Mellitus (T2DM), a chronic disorder of carbohydrate, fat, and protein metabolism, is an important cause of morbidity and mortality in the US. Like BPH/LUTD, T2DM is associated with older age, as well as with obesity, a family history of diabetes, a history of gestational diabetes, impaired glucose metabolism, physical inactivity, and race/ethnicity [5]. The National Institute of Diabetes and Digestive and Kidney Diseases (NIDDK) reports that T2DM currently affects 25.8 million people of all ages, or 8.3%, of the entire US population. In 2010, the most recent year for which there is data, 10.9 million (26.9%) of all US residents aged 65 years or older had T2DM, and 1.9 million people aged 20 years or older were newly diagnosed with T2DM [6].

There is growing evidence that LUTD and T2DM are linked etiologically and biologically. Diet-induced obesity has been identified as a risk factor for both T2DM and LUTS in men [7,8]. Conversely, reversion of obesity through weight loss is linked with reduction of symptoms associated with diabetes and LUTS [9]. Several epidemiologic studies that have examined the association between LUTS and diabetes also suggest that LUTS may occur more frequently among men with diabetes, with an estimated 25% to nearly twofold increased risk of LUTS in men with diabetes [10–13]. In addition, among 9,856 men with clinically diagnosed BPH, the presence of diabetes (13%) was associated with increased LUTS severity, affecting voiding more than storage function. Patients with BPH and diabetes had a significantly higher baseline International Prostate Symptoms Score (IPSS) and a significantly lower maximal urinary flow rate (Q_{max}) that those without diabetes (both $P < 0.001$) [12].

A possible explanation for an association between BPH and diabetes beyond that explained by comorbidity due to age is that the two disease states can cause at least partially similar urological symptoms. However, the underlying biological mechanisms producing these symptoms may be different. Dib et al. studies 50 consecutive diabetic patients, 23 (46%) of whom had concurrent BOO symptoms based on pressure/flow urodynamic measurements. However, no significant differences in IPSS or prostate volume were apparent between diabetic patients with BOO compared to those without obstructive symptoms. These data suggest little, if any, association between BOO in diabetic patients with prostate enlargement and LUTS [14]. Similarly, a multiethnic community-based study demonstrated positive associations between diabetes and irritative LUTS and nocturia, but not between diabetes

across measures more specific to BPH (i.e., prostate volume, PSA, and peak urinary flow rate) [15]. Taken together, these studies suggest that the presence of diabetes may be less related to prostate growth and more related to the dynamic components of lower urinary tract function.

We have previously reported that progressive aging- and inflammation-associated fibrosis effectively remodels the extracellular matrix (ECM) to increase prostate tissue stiffness and reduce urethral flexibility, resulting in urinary flow obstruction and LUTS [16]. These observations suggest that tissue fibrosis adversely changes the dynamic of lower urinary tract function. In the current study, we sought to test these associations in a mouse model of accelerated aging subjected to diet-induced obesity and T2DM. Specifically, the studies reported here were designed to test whether senescence-accelerated mouse prone (SAMP)6 mice, which were reported to develop prostatic fibrosis [17–20], would also develop LUTS, and whether these symptoms would be exacerbated by diet-induced obesity and concurrent T2DM. The results of these studies show that SAMP6 mice and AKR/J background strain mice develop diet-induced obesity and T2DM concurrent with urinary voiding dysfunction. Moreover, urinary voiding dysfunction is more severe in SAMP6 mice and is associated with pronounced prostatic and urethral fibrosis. Taken together, these studies suggest that obesity, T2DM, lower urinary tract fibrosis, and urinary voiding dysfunction are inextricably and biologically linked.

MATERIALS AND METHODS

Mouse Strains and Maintenance

Two related mouse strains were used in these studies: SAMP6 and the AKR/J background strain. Colonies were established from eight females and four males per strain purchased at 6 weeks of age (Harlan Laboratories, Indianapolis, IN). At 6–8 weeks of age, 25 mice each SAMP6 and AKR/J were fed the following diets: high fat diet (HFD) containing 60% calories from fat, 20% protein, and 20% carbohydrates (58Y1, Test Diet, Richmond, IN); low fat diet (LFD) containing 10.2% calories from fat, 18.3% protein, and 71.5% carbohydrates (58Y2, Test Diet, Richmond, IN), or regular diet (RD) grain-based mouse chow containing 13.50% calories from fat, 28.50% protein, and 58% carbohydrates (#5001, Lab Diet, St. Louis, MO). The mice were fed daily with fresh high, low fat or regular chow (5 g/day) for 8 months. Mice were housed in the Unit for Animal Laboratory Medicine (ULAM) facility at the University of Michigan under enriched conditions at a constant temperature (22–23°C) with a 12/12 hr light/dark cycle and optimal humidity and free access to tap water and food ad libitum. The body weights of all mice were measured once during the first week of the month for eight consecutive months. All animal procedures were performed using protocols approved by the University Committee on Use and Care of Animals (UCUCA).

Oral Glucose Tolerance Test

Oral glucose tolerance tests (OGTTs) were carried out just prior to the termination of the study. OGTTs were measured in 10 mice each fed HFD or LFD from each mouse strain (a total of 40 mice). The OGTTs were performed in semi-fasted mice, for example, on the day

preceding the test, mice fasted for 5 hr, starting at 8:30 am. Glucose 50% was given around 1:30 pm via oral gavage at 2.0 g/kg. Blood samples were collected prior to and after the gavage at the time of 0, 15, 30, 60, and 120 min after via tail vein bleeding. The oral glucose load was given by gavage via a gastric tube connected to a syringe to ensure accurate dosing. Blood glucose concentration was measured at all-time points using a glucometer (Acucheck, Roche).

Plasma Insulin Measurement

Blood samples were collected in tubes containing EDTA to avoid clotting and placed on ice until they were centrifuged at 3,000 rpm and frozen at −80°C until plasma content measurements were conducted. Plasma levels of insulin were determined using millipore rat/mouse insulin using a commercially available insulin ELISA kit [12]. Animals were restrained repeatedly for less than a minute each time while blood samples were collected.

Determination of Urinary Voiding Function

The urinary voiding function of all of mice were measured once during the first week of the month for eight consecutive months. The urinary voiding function was determined using a filter paper assay, as previously described with some modification [21]. For these studies, all mice in a single cage (4–5 mice) were placed into a urine monitoring cage. The bottom of this cage was fitted with a wire mesh beneath which was What man Grade 3 filter paper. The mice were left in the monitoring cage for 5 hr, after which the filter paper was collected. Urine which had soaked into the filter paper was strongly fluorescent under UV light and was easily visualized under those conditions. The pattern of urine spots was independently determined by two different observers (M. G.-K. and J. R.-N.) using a modification of previously described methods [21]. Each voiding pattern was given a grade of 1–5 depending upon the size and number of urine spots such that a score of 1 indicated the observation of single, large urine spots (no voiding dysfunction) and a score of 5 indicated the observation of many small, scattered urine spots (obstructive voiding dysfunction). The data from the two independent observers was averaged and statistically analyzed.

Tissue Processing and Histological Evaluation

Mouse lower urinary tracts were harvested at 10 months of age (after 8 months of feeding with RD, HFD, or LFD). Male mice were euthanized by CO_2 asphyxiation in accordance with institutional guidelines. Lower urinary tracts consisting of bladder, prostatic and pelvic urethra, prostate and seminal vesicles were ressected *en bloc* and placed in ice cold saline. Peripheral adipose tissue was removed and distal prostate lobe aspects were teased apart to liberate each from its attachments to other prostate lobes, seminal vesicle, and urethra. To preserve proximodistal orientation of seminal vesicle and prostate ducts, lower urinary tract tissues were fixed intact by orienting them on their lateral surfaces, sandwiching them between histology sponges and fixing them overnight at 4°C in 10% neutral buffered formalin. Histology sponges were removed and tissues were dehydrated through an ethanol series, cleared in xylene and infiltrated with paraffin. Tissue sections were subjected to hematoxylin/eosin (H/E) staining and assessed for histopathology or subjected to Masson's Trichrome staining to assess collagen content. Prostate wet weight was not measured because of inherent variability in prostate morphology in the different strains.

Collagen Content

Collagen content was determined using the methodology described previously [16,22]. Briefly, Masson's Trichrome stained tissue sections were digitally imaged using a PathScan Enabler IV and color segmented using a subprogram within MATLAB (R2010a; MathWorks, Natick, MA) that separates and quantifies color elements from trichrome images, permitting quantitation of blue-stained areas corresponding to extracellular collagen. Using the area of a single tissue section as the denominator, this approach provides a means to calculate the portion of this area that is made up by mature extracellular collagen I (the numerator), hence, the percentage of extracellular collagen type I (numerator/denominator × 100) in that tissue section. By extension, this method also permits calculation of the percentage of the entire piece of tissue that is made up of mature extracellular collagen I.

Statistical Analysis

Averages and standard deviations were calculated and compared using two-tailed Students' *t*-tests. In all tests, $P < 0.05$ was considered statistically significant.

RESULTS

High Fat Diet-Fed Mice Develop Obesity-Induced Type 2 Diabetes Mellitus

Both SAMP6 (Fig. 1A,C) and AKR/J (Fig. 1B,D) mice demonstrated cumulative weight gains of 1–2 g and 5–7 g when fed a RD or LFD over an 8-month period, respectively. In contrast, SAMP6 (Fig. 1A,C) and AKR/J (Fig. 1B,D) mice almost doubled in body weight, from ~30 g at the initiation of a HFD to a total body weight of 50–60 g (cumulative weight gain of 20–30 g), when fed a HFD over an 8-month period.

At the end of 8 months, SAMP6 and AKR/J mice fed continuously either the LFD or HFD were subjected to 2 hr OGTTs. The results of the OGTTs showed that SAMP6 HFD-fed mice demonstrated the highest blood glucose levels, which peaked at 420 mg/dl at 40 min, followed by SAMP6 LFD-fed mice (300 mg/dl glucose), AKR/J HFD-fed mice (220 mg/dl) and AKR/J LFD-fed mice (200 mg/dl) (Fig. 2A). The average areas under the curve (AUCs) demonstrated significantly higher blood glucose levels for SAMP6 HFD-fed compared to LFD-fed mice ($P < 0.0003$), and AKR/J HFD-fed compared to LFD-fed mice ($P < 0.03$) (Fig. 2B). The AUCs also showed that blood glucose levels were significantly higher for SAMP6 HFD-fed compared to AKR/J HFD-fed ($P < 0.001$) and for SAMP6 LFD-fed compared to AKR/J LFD-fed ($P < 0.04$) mice. Plasma insulin levels were determined concurrent with the blood glucose levels. The results of these studies showed that plasma insulin levels were significantly higher for SAMP6 compared to AKR/J HFD-fed mice ($P < 0.001$), for SAMP6 HFD-fed compared to LFD-fed mice ($P < 0.001$) and for AKR/J HFD-fed compared to LFD-fed mice ($P < 0.002$) (Fig. 2C,D).

Taken together, these data suggest that both SAMP6 and AKR/J HFD-fed mice developed hyperglycemia and insulin resistance (hyperinsulinemia) consistent with T2DM concurrent with diet-induced obesity.

High Fat Diet-Fed Mice Develop Urinary Voiding Dysfunction

Several epidemiologic studies have linked LUTS with T2DM [9–12]. Therefore, we examined both HFD-fed and LFD-fed mice for urinary voiding function. For these studies, all mice in a single cage (4–5 mice) were placed into a urine monitoring cage for 5 hr and the pattern of urine spots on the filter paper visualized under UV light. The pattern of urine spots was assessed using a modification of previously described methods by two different observers and the results averaged and statistically analyzed. As shown in Figure 3A, the urinary voiding pattern was graded on a scale of 1–5 depending upon the size and number of urine spots such that a score of 1 indicated the observation of single, large urine spots (no voiding dysfunction) and a score of 5 indicated the observation of many small, scattered urine spots (obstructive voiding dysfunction). Urine voiding patterns were assessed for SAMP6 and AKR/J mice after 7 and 8 months of continuous feeding on RD, LFD, or HFD. Both SAMP6 and AKR/J mice demonstrated normal urinary voiding patterns after 7 or 8 months continuous RD-feeding. SAMP6 and AKR/J mice demonstrated similar though slightly abnormal urinary voiding patterns suggestive of mild obstruction at 7 and 8 months continuous LFD-feeding. Both SAMP6 and AKR/J mice demonstrated abnormal urinary voiding patterns suggestive of moderate obstruction for AKR/J mice and moderate/severe obstruction for SAMP6 mice at 7 and 8 months continuous HFD-feeding. The urine voiding scores for both SAMP6 and AKR/J HFD-fed mice were significantly worse than for LFD-fed ($P < 0.008$) and RD-fed mice ($P < 0.001$). Further, SAMP6 urinary voiding dysfunction was significantly worse ($P < 0.001$) than that of AKR/J mice at both 7 and 8 months continuous HFD-feeding (Fig. 3B). In addition to dermatitis, both SAMP6 and AKR/J HFD-fed mice exhibited acute urinary retention and were unable to void urine, requiring euthanasia (Fig. 4A,B). The results of these studies demonstrate that continuous feeding on a HFD was associated with the acquisition of urinary voiding dysfunction for both SAMP6 and AKR/J mice, but the level of dysfunction was most severe for SAMP6 HFD-fed mice.

HFD-Fed Mice Exhibit Lower Urinary Tract Fibrosis

Previous studies from our group showed that the peri-urethral prostate tissues from men with LUTS were significantly stiffer ($P = 0.0016$, r = 0.82) and demonstrated significantly higher collagen content ($P = 0.0038$, r = 0.60) and lower glandularity than those from men without LUTS [16]. These observations suggested that ECM deposition and fibrosis contribute to urinary obstructive symptoms and LUTS. Therefore, we examined the lower urinary tract tissues of LFD-fed and HFD-fed mice for histopathological evidence of fibrosis. Masson's Trichrome stained tissue sections of fixed and embedded mouse lower urinary tracts (Fig. 5A) were digitally imaged and color segmented using a subprogram within MATLAB that separates and quantifies color elements from images of stained tissues, permitting quantitation of blue-stained areas corresponding to extracellular collagen [16,23]. Because previous studies had suggested that SAMP6 mice exhibited fibrosis of the dorsal lobe [19] we specifically focused on analyzing the collagen content of the dorsal lobe. Although the urethral region presented as a saggital, rather than the desired coronal, cross-sectional area in these particular preparations of the lower urinary tract, these were also analyzed for collagen content. As shown in Figure 5B, the prostatic dorsal lobes of SAMP6 ($P < 0.001$) and AKR/J ($P < 0.01$) HFD-fed mice demonstrated 2–4 × higher collagen content than those of LFD-fed mice ($P < 0.001$). Similarly, the urethral regions of SAMP6 ($P < 0.001$) and AKR/J

($P < 0.001$) HFD-fed mice ($P < 0.003$) demonstrated 2–4 × higher collagen levels than those of LFD-fed mice.

Histopathological analysis of serial H/E stained sections to those analyzed for collagen content demonstrated peri-glandular prostatic fibrosis in SAMP6 HFD-fed mice (Fig. 5C, i and ii) and milder focal fibroplasia in SAMP6 LFD-fed mice (Fig. 5C, iii and iv). These differences in peri-glandular fibrosis were more evident in SAMP6 HFD-fed than LFD-fed mice, and these differences trended towards, but did not reach, statistical significance ($P = 0.10$) (Table I). Epithelial hyperplasia was more evident in AKR/J HFD-fed and LFD-fed mice than SAMP6 mice, but the observed differences between diets (for either strain) were not significant (Table I). The anterior prostates appeared normal in both HFD-fed and LFD-fed SAMP6 and AKR/J mice, as did the seminal vesicles though some mild epithelial hyperplasia was observed for AKR/J (not shown). Notably, significantly higher levels of brown adipose tissue (BAT) than white adipose tissue (WAT) was evident in SAMP6 LFD-fed compared to HFD-fed mice ($P = 0.005$) (Table I) (Fig. 5D). A similar trend was noted for AKR/J LFD-fed compared to HFD-fed mice but these differences did not reach significance (Table I).

DISCUSSION

Previous studies from our research group showed that lower urinary tract fibrosis is associated with moderate/severe LUTS in American men [16]. The studies reported here now show that SAMP6 mice and AKR/J background strain mice develop diet-induced obesity and T2DM concurrent with urinary voiding dysfunction and pronounced lower urinary tract fibrosis. Taken together, these studies suggest that obesity, T2DM, lower urinary tract fibrosis, and urinary voiding dysfunction are inextricably and biologically linked.

Both the human and mouse studies point to inflammation as a common biological link between lower urinary tract fibrosis, LUTD, obesity, and T2DM. Several studies have shown that male LUTD is associated with inflammation of the prostate, evident as prostatic inflammatory infiltrate and/or prostatitis. Immunohistochemical studies examining the histopathology of BPH have reported the presence of pervasive inflammatory infiltrate comprising leukocytes associated with acute inflammation, chronic inflammation, or both. Inflammatory cells comprising neutrophillic or lymphocytic infiltrates were identified in 90% of transurethral resections of the prostate (TURP) specimens from 80 patients diagnosed with BPH/LUTS but no history of prostatitis or prostatic infection [24]. Chronic inflammatory infiltrate was also detected in 30–60% of 1,197 randomly selected men with BPH/ LUTS as part of the Medical Therapy of Prostatic Symptoms (MTOPS) study. Patients with chronic inflammatory infiltrate had larger prostate volumes and demonstrated significantly more clinical progression and acute urinary retention than those with no evidence of inflammation [25,26]. A study that prospectively analyzed 167 autopsied prostates identified 93 glands harboring BPH/LUTS, and 75% of these demonstrated inflammatory infiltrate (predominantly chronic inflammation) compared to 50% of those without BPH/LUTS and 55% of those with evidence of cancer [27]. As originally reported by Theyer et al. [28] and Steiner et al. [29] and recently summarized by Kramer et al. [30],

inflammatory infiltrates are very commonly observed in BPH/LUTS specimens and comprise 70% T-lymphocytes, 15% B cells, and 15% macrophages, as well as mast cells. These studies also showed that resident T-lymphocyte populations in prostate tissues actively secrete a diverse array of chemokines into the surrounding microenvironment, including those known to strongly induce myofibroblast differentiation and therefore potentiate fibrosis.

Studies from our own laboratory have shown that the aging human prostate is characterized by an inflammatory tissue microenvironment. CXCL8 (IL-8) and a closely related CXC-type chemokine, CXCL5 (ENA-78), are secreted at significantly higher levels by stromal fibroblasts cultured from the prostates of older compared to younger men [31–33]. Moreover, these and additional chemokines (CXCL1, CXCL6, CXCL12) secreted by aging prostate stroma induced proliferative responses from both epithelial and stromal prostate cells in vitro [32,34,35]. Studies published by the Rowley laboratory have shown that myofibroblast-rich “reactive stroma” characterizes hyperplastic, dysplastic, and neoplastic-associated prostatic stroma [36,37], that BPH nodules exhibited elevated epithelial CXCL8 immunoreactivity associated with reactive stroma [37], that CXCL8 was sufficient for induction of a fibroblast to myofibroblast transition [37], and that over-expression of KC, the mouse homologue of CXCL8, in mouse prostatic epithelium was sufficient to produce hyperplastic prostate epithelial acini associated with a periacinar reactive stroma [38].

In addition to low-level, but persistent, chronic inflammation and aging-associated inflammatory changes in the tissue microenvironment, obesity likely contributes significantly to inflammatory changes in adjacent tissues. Obesity-mediated inflammatory changes in the tissue microenvironment, or “metainflammation,” [39] include those produced by adipocytes and resident macrophages in WAT. In addition to triglyceride and lipid storage, WAT adipocytes secrete a medley of endocrine and paracrine factors, collectively termed adipokines, which include inflammatory mediators such as interleukins, CC- and CXC-type chemokines, and TGF-β [40,41]. As reported here, significantly higher levels of WAT were evident for HFD-fed compared to LFD-fed mice in association with lower urinary tract fibrosis and urinary voiding dysfunction.

The level and composition of inflammatory adipokines is altered in obesity-associated WAT [41], and some of these are known to activate the IKKβ/NF-κB pathway in adipocytes, hepatocytes, and associated macrophages. NF-κB is a powerful transcription factor that mediates the expression of multiple genes encoding inflammatory mediators, including several interleukins, CC- and CXC-type chemokines, and TGF-β [42,43]. TGF-β is a well-known pro-fibrotic protein that promotes myofibroblast phenoconversion and tissue fibrosis [44,45]. A recent study reported that adipose tissue from obese subjects contained increased areas of fibrosis, which correlated inversely with insulin and positively with macrophage number, compared to adipose tissue from lean subjects. Although macrophages in crownlike structures (CLS) were more abundant in obese adipose tissue, the majority of macrophages were associated with fibrosis and were not organized in CLS. Macrophages in CLS were predominantly M1, but most other macrophages, particularly those in fibrotic areas, were M2. Moreover, TGF-β was more abundant in M2 macrophages and was further increased by coculture with adipocytes. Downstream effectors of TGF-β, such as plasminogen activator

in-hibitor-1, collagen VI, and phosphorylated Smad, were increased in macrophages and adipocytes. Thus, adipose tissue of insulin-resistant humans demonstrated increased fibrosis, M2 macrophage abundance, and TGF-β activity [46]. Recent studies from our research group show that several CXC-type chemokines, notably CXCL5, CXCL8, and CXCL12, can mediate myofibroblast phenoconversion and accumulation in the absence of TGF-β [47]. Taken together, these studies suggest that inflammatory changes in the tissue microenvironment brought about through low level but chronic infiltration by the innate immune system, aging, and/or obesity may be sufficient to promote myofibroblast phenoconversion, accumulation, and fibrosis in affected tissues, including those of the lower urinary tract.

The studies reported here utilized the SAMP mouse model, which was developed through inbreeding of AKR/J mice as a model of spontaneous senescence in mice. The aging pattern in this model is considered to be due to an accelerated senescence rather than to premature aging or senescence [19,48]. An early study noted that the most striking histological changes in SAMP6 mouse prostates were stromal hyperplasia and inflammation in the dorsal prostate at age 15 months [19]. Moreover, regular mouse chow-fed SAMP6 mice exhibit higher levels of plasma glucose, triglyceride, insulin, and leptin levels and hepatic lipid levels, but lower levels of plasma glucagon and adiponectin, than age-matched AKR/J mice [20]. These observations suggest that SAMP6 mice may be predisposed to developing hyperglycemia and insulin resistance consistent with T2DM. Indeed, the results of the studies reported here support this conclusion and show that HFD-fed SAMP6 mice exhibited higher levels of hyperglycemia and insulin resistance concurrent with worse lower urinary tract fibrosis and dysfunction compared to HFD-fed AKR/J mice.

In summary, the studies reported here demonstrate the acquisition of urinary voiding dysfunction concurrent with obesity-induced T2DM and lower urinary tract fibrosis in a mouse model. This model recapitulates several epidemiological studies of human populations that associate obesity, metabolic syndrome, and T2DM with urinary voiding dysfunction. Therefore, further studies using these mouse models may provide the means to delineate the cellular mechanisms that biologically couple lower urinary tract fibrosis and urinary voiding dysfunction with obesity-induced T2DM.

Acknowledgments

We would like to thank Dr. Jeremy Adler for his help assessing lower urinary tract tissues collagen content. This work was funded by the National Institutes of Health (NIH)/National Institute of Diabetes and Digestive and Kidney Diseases (NIDDK) Award P20DK090770 (J.A.M.) and by the Michigan Institute for Clinical & Health Research (MICHR) NIH Clinical & Translational Science Award (CTSA) UL1RR024986 (M.G.-K.).

References

1. Meigs JB, Mohr B, Barry MJ, Collins MM, McKinlay JB. Risk factors for clinical benign prostatic hyperplasia in a community-based population of healthy aging men. J Clin Epidemiol. 2001; 54(9): 935–944. [PubMed: 11520654]
2. Verhamme KM, Dieleman JP, Bleumink GS, van der Lei J, Sturkenboom MC, Artibani W, Begaud B, Berges R, Borkowski A, Chappel CR, Costello A, Dobronski P, Farmer RD, Jimenez Cruz F, Jonas U, MacRae K, Pientka L, Rutten FF, van Schayck CP, Speakman MJ, Tiellac P, Tubaro A, Vallencien G, Vela Navarrete R. Incidence and prevalence of lower urinary tract symptoms

suggestive of benign prostatic hyperplasia in primary care—The Triumph project. Eur Urol. 2002; 42(4):323–328. [PubMed: 12361895]

3. Guess HA. Benign prostatic hyperplasia: Antecedents and natural history. Epidemiol Rev. 1992; 14:131–153. [PubMed: 1283852]
4. McVary KT. A review of combination therapy in patients with benign prostatic hyperplasia. Clin Ther. 2007; 29(3):387–398. [PubMed: 17577460]
5. Garber AJ. Obesity and type 2 diabetes: Which patients are at risk? Diabetes Obes Metab. 2012; 14(5):399–408. [PubMed: 22074144]
6. Centers for Disease Control and Prevention National Diabetes Fact Sheet. National estimates and general information on diabetes and prediabetes in the United States 2011. Atlanta, GA: US Department of Health and Human; Services, Centers for Disease Control and Prevention; 2011.
7. Parsons JK. Benign prostatic hyperplasia and male lower urinary tract symptoms: Epidemiology and risk factors. Curr Bladder Dysfunct Rep. 2010; 5(4):212–218. [PubMed: 21475707]
8. Parsons JK, Sarma AV, McVary K, Wei JT. Obesity and benign prostatic hyperplasia: Clinical connections, emerging etiological paradigms and future directions. J Urol. 2013; 189(1 Suppl):S102–S106. [PubMed: 23234610]
9. Khoo J, Piantadosi C, Duncan R, Worthley SG, Jenkins A, Noakes M, Worthley MI, Lange K, Wittert GA. Comparing effects of a low-energy diet and a high-protein low-fat diet on sexual and endothelial function, urinary tract symptoms, and inflammation in obese diabetic men. J Sex Med. 2011; 8(10):2868–2875. [PubMed: 21819545]
10. Klein BE, Klein R, Lee KE, Bruskewitz RC. Correlates of urinary symptom scores in men. Am J Public Health. 1999; 89(11):1745–1748. [PubMed: 10553401]
11. Joseph MA, Harlow SD, Wei JT, Sarma AV, Dunn RL, Taylor JM, James SA, Cooney KA, Doerr KM, Montie JE, Schottenfeld D. Risk factors for lower urinary tract symptoms in a population-based sample of African-American men. Am J Epidemiol. 2003; 157(10):906–914. [PubMed: 12746243]
12. Michel MC, Mehlburger L, Schumacher H, Bressel HU, Goepel M. Effect of diabetes on lower urinary tract symptoms in patients with benign prostatic hyperplasia. J Urol. 2000; 163(6):1725–1729. [PubMed: 10799169]
13. Koskimaki J, Hakama M, Huhtala H, Tammela TL. Association of non-urological diseases with lower urinary tract symptoms. Scand J Urol Nephrol. 2001; 35(5):377–381. [PubMed: 11771864]
14. Dib PT, Trigo-Rocha F, Gomes CM, Srougi M. Urodynamic evaluation in diabetic patients with prostate enlargement and lower urinary tract symptoms. Urol Int. 2008; 80(4):378–382. [PubMed: 18587248]
15. Sarma AV, Burke JP, Jacobson DJ, McGree ME, St Sauver J, Girman CJ, Lieber MM, Herman W, Macoska J, Montie JE, Jacobsen SJ. Associations between diabetes and clinical markers of benign prostatic hyperplasia among community-dwelling Black and White men. Diabetes Care. 2008; 31(3):476–482. [PubMed: 18071006]
16. Ma J, Gharaee-Kermani M, Kunju L, Hollingsworth JM, Adler J, Arruda EM, Macoska JA. Prostatic fibrosis is associated with lower urinary tract symptoms. J Urol. 2012; 188(4):1375–1381. [PubMed: 22906651]
17. Takeda T, Hosokawa M, Higuchi K. Senescence-accelerated mouse (SAM): A novel murine model of senescence. Exp Gerontol. 1997; 32(1–2):105–109. [PubMed: 9088907]
18. Takeda T, Matsushita T, Kurozumi M, Takemura K, Higuchi K, Hosokawa M. Pathobiology of the senescence-accelerated mouse (SAM). Exp Gerontol. 1997; 32(1–2):117–127. [PubMed: 9088909]
19. Sugimura Y, Sakurai M, Hayashi N, Yamashita A, Kawamura J. Age-related changes of the prostate gland in the senescence-accelerated mouse. Prostate. 1994; 24(1):24–32. [PubMed: 7507239]
20. Niimi K, Takahashi E, Itakura C. Adiposity-related biochemical phenotype in senescence-accelerated mouse prone 6 (SAMP6). Comp Med. 2009; 59(5):431–436. [PubMed: 19887026]
21. Hodges SJ, Zhou G, Deng FM, Aboushwareb T, Turner C, Andersson KE, Santago P, Case D, Sun TT, Christ GJ. Voiding pattern analysis as a surrogate for cystometric evaluation in uroplakin II knockout mice. J Urol. 2008; 179(5):2046–2051. [PubMed: 18355864]

22. Adler J, Swanson SD, Schmiedlin-Ren P, Higgins PD, Golembeski CP, Polydorides AD, McKenna BJ, Hussain HK, Verrot TM, Zimmermann EM. Magnetization transfer helps detect intestinal fibrosis in an animal model of Crohn disease. Radiology. 2011; 259(1):127–135. [PubMed: 21324841]
23. Adler. Imatinib decreases bowel wall fibrosis, reduces inflammatory cytokines and pro-fibrotic factors in peptidoglican-polysaccharide rat model of Crohn's disease. 2010
24. Nickel JC, Downey J, Young I, Boag S. Asymptomatic inflammation and/or infection in benign prostatic hyperplasia. BJU Int. 1999; 84(9):976–981. [PubMed: 10571623]
25. Roehrborn C, Kaplan S, Noble W, Lucia M, Slawin K, McVary K, Kusek J, Nyberg L. The impact of acute or chronic inflammation in baseline biopsy on the risk of clinical progression of BPE: Results from the MTOPS study. AUA Meeting. 2005 Abstract # 1277.
26. Robert G, Descazeaud A, Nicoläıew N, Terry S, Sirab N, Vacherot F, Maille´ P, Allory Y, de la Taille A. Inflammation in benign prostatic hyperplasia: A 282 patients' immunohistochemical analysis. Prostate. 2009; 69(16):1774–1780. [PubMed: 19670242]
27. Delongchamps NB, de la Roza G, Chandan V, Jones R, Sunheimer R, Threatte G, Jumbelic M, Haas GP. Evaluation of prostatitis in autopsied prostatesis chronic inflammation more associated with benign prostatic hyperplasia or cancer? J Urol. 2008; 179(5):1736–1740. [PubMed: 18343414]
28. Theyer G, Kramer G, Assmann I, Sherwood E, Preinfalk W, Marberger M, Zechner O, Steiner GE. Phenotypic characterization of infiltrating leukocytes in benign prostatic hyperplasia. Lab Invest. 1992; 66(1):96–107. [PubMed: 1370561]
29. Steiner GE, Stix U, Handisurya A, Willheim M, Haitel A, Reithmayr F, Paikl D, Ecker RC, Hrachowitz K, Kramer G, Lee C, Marberger M. Cytokine expression pattern in benign prostatic hyperplasia infiltrating T cells and impact of lymphocytic infiltration on cytokine mRNA profile in prostatic tissue. Lab Invest. 2003; 83(8):1131–1146. [PubMed: 12920242]
30. Kramer G, Mitteregger D, Marberger M. Is benign prostatic hyperplasia (BPH) an immune inflammatory disease? Eur Urol. 2007; 51(5):1202–1216. [PubMed: 17182170]
31. Begley L, Monteleon C, Shah RB, Macdonald JW, Macoska JA. CXCL12 overexpression and secretion by aging fibroblasts enhance human prostate epithelial proliferation in vitro. Aging Cell. 2005; 4(6):291–298. [PubMed: 16300481]
32. Begley LA, Kasina S, MacDonald J, Macoska JA. The inflammatory microenvironment of the aging prostate facilitates cellular proliferation and hypertrophy. Cytokine. 2008; 43(2):194–199. [PubMed: 18572414]
33. Macoska JA. Chemokines and BPH/LUTS. Differentiation. 2011; 82(4–5):253–260. [PubMed: 21600689]
34. Begley LA, Kasina S, Mehra R, Adsule S, Admon AJ, Lonigro RJ, Chinnaiyan AM, Macoska JA. CXCL5 promotes prostate cancer progression. Neoplasia. 2008; 10(3):244–254. [PubMed: 18320069]
35. Begley LA, MacDonald JW, Day ML, Macoska JA. CXCL12 activates a robust transcriptional response in human prostate epithelial cells. J Biol Chem. 2007; 282(37):26767–26774. [PubMed: 17631494]
36. Tuxhorn JA, Ayala GE, Smith MJ, Smith VC, Dang TD, Rowley DR. Reactive stroma in human prostate cancer: induction of myofibroblast phenotype and extracellular matrix remodeling. Clin Cancer Res. 2002; 8(9):2912–2923. [PubMed: 12231536]
37. Schauer IG, Ressler SJ, Tuxhorn JA, Dang TD, Rowley DR. Elevated epithelial expression of interleukin-8 correlates with myofibroblast reactive stroma in benign prostatic hyperplasia. Urology. 2008; 72(1):205–213. [PubMed: 18314176]
38. Schauer IG, Ressler SJ, Rowley DR. Keratinocyte-derived chemokine induces prostate epithelial hyperplasia and reactive stroma in a novel transgenic mouse model. Prostate. 2009; 69(4):373–384. [PubMed: 19021203]
39. Lumeng CN, Saltiel AR. Inflammatory links between obesity and metabolic disease. J Clin Invest. 2011; 121(6):2111–2117. [PubMed: 21633179]
40. Harwood HJ Jr. The adipocyte as an endocrine organ in the regulation of metabolic homeostasis. Neuropharmacology. 2012; 63(1):57–75. [PubMed: 22200617]

41. Taube A, Schlich R, Sell H, Eckardt K, Eckel J. Inflammation and metabolic dysfunction: Links to cardiovascular diseases. Am J Physiol Heart Circ Physiol. 2012; 302(11):H2148–H2165. [PubMed: 22447947]

42. Pahl HL. Activators and target genes of Rel/NF-kappaB transcription factors. Oncogene. 1999; 18(49):6853–6866. [PubMed: 10602461]

43. Shoelson SE, Lee J, Goldfine AB. Inflammation and insulin resistance. J Clin Invest. 2006; 116(7): 1793–1801. [PubMed: 16823477]

44. Scotton CJ, Chambers RC. Molecular targets in pulmonary fibrosis: The myofibroblast in focus. Chest. 2007; 132(4):1311–1321. [PubMed: 17934117]

45. Wynn TA. Cellular and molecular mechanisms of fibrosis. J Pathol. 2008; 214(2):199–210. [PubMed: 18161745]

46. Spencer M, Yao-Borengasser A, Unal R, Rasouli N, Gurley CM, Zhu B, Peterson CA, Kern PA. Adipose tissue macrophages in insulin-resistant subjects are associated with collagen VI and fibrosis and demonstrate alternative activation. Am J Physiol Endocrinol Metab. 2010; 299(6):E1016–E1027. [PubMed: 20841504]

47. Gharaee-Kermani M, Kasina S, Moore BB, Thomas D, Mehra R, Macoska JA. CXC-type chemokines promote myofibroblast phenoconversion and prostatic fibrosis. PLoS ONE. 2012; 7(11):e49278. [PubMed: 23173053]

48. Lecka-Czernik B, Moerman EJ, Shmookler Reis RJ, Lipschitz DA. Cellular molecular biomarkers indicate precocious in vitro senescence in fibroblasts from SAMP6 mice. Evidence supporting a murine model of premature senescence and osteopenia. J Gerontol A Biol Sci Med Sci. 1997; 52(6):B331–B336. [PubMed: 9402934]

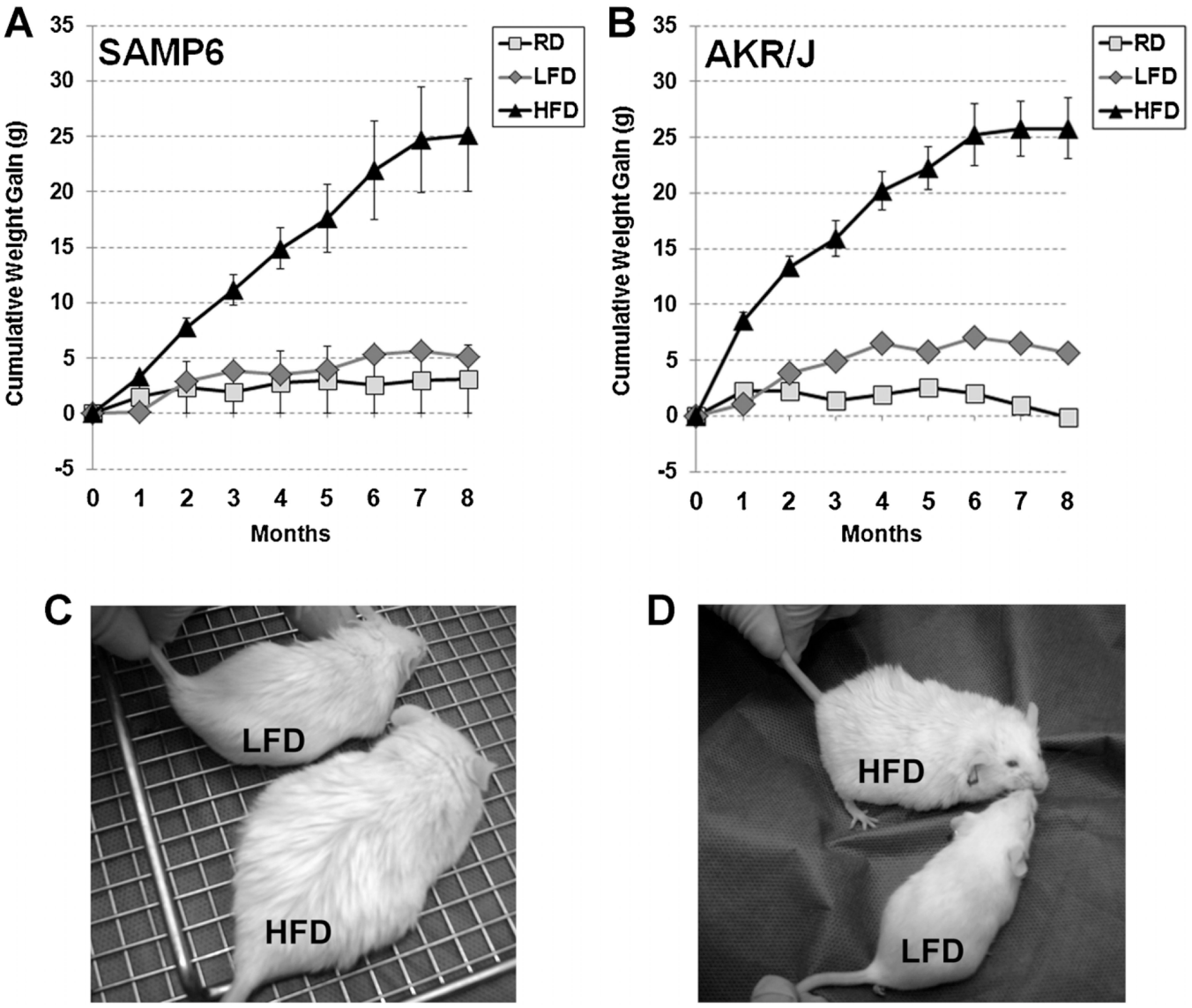

Fig. 1.

High fat diet-induced obesity in SAMP6 and AKR/J Mice. The graphs depict the cumulative weight gain of SAMP6 (**A**) and AKR/J (**B**) mice fed regular mouse chow diet (RD), low fat diet (LFD) or high fat diet (HFD) for 8 months. Mice from both strains fed RD or LFD gained 1–5 g over the 8-month period whereas those fed HFD virtually doubled in weight and gained 20–30 g over the same period. Photographs depict representative SAMP6 (**C**) and AKR/J(**D**) mice after 8 months on LFD or HFD diets as indicated.

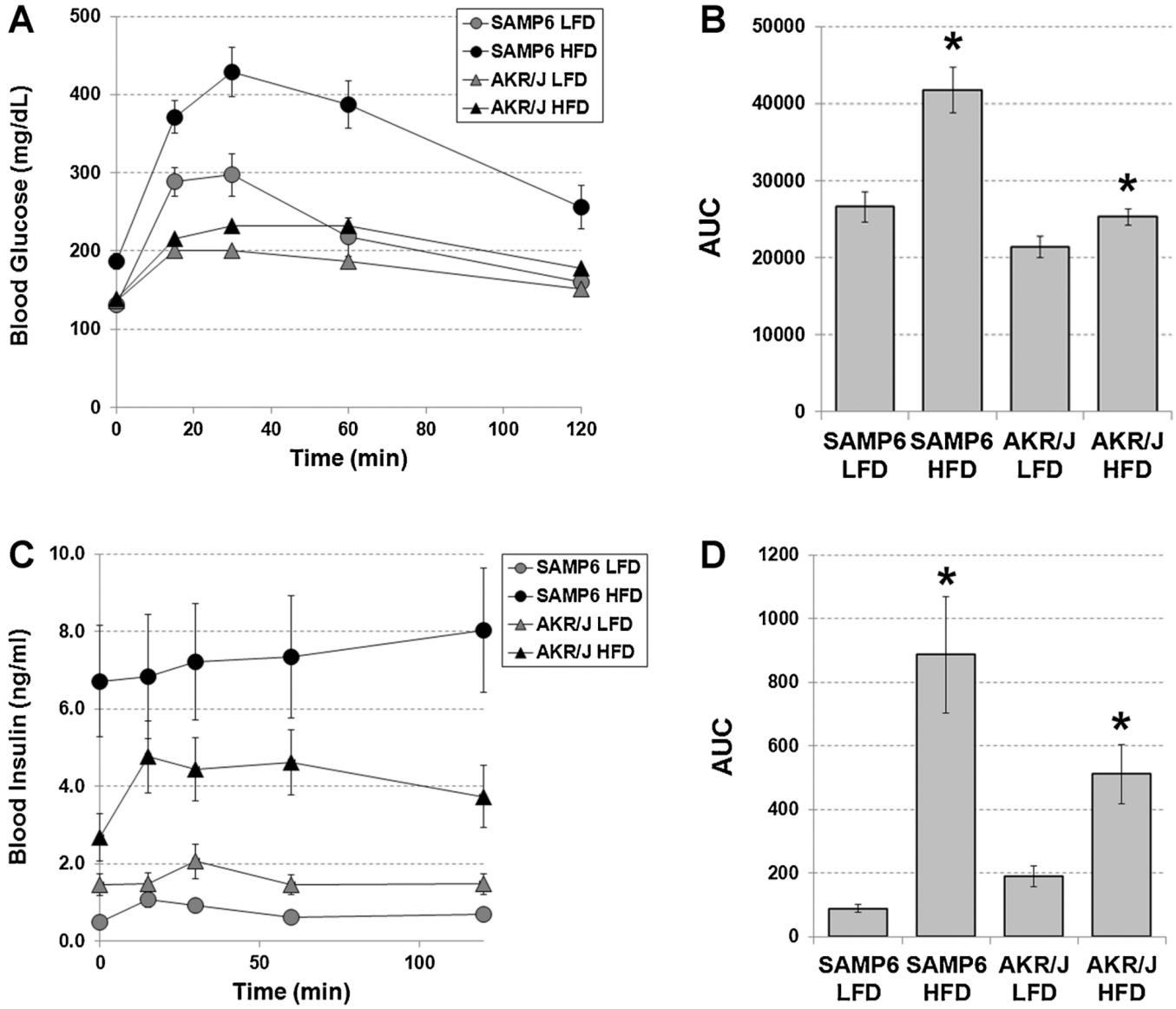

Fig. 2.

SAMP6 and AKR/J mice HFD-fed mice develop hyperglycemia and insulin resistance consistent with T2DM. **A**: At the end of 8 months, SAMP6 and AKR/J mice fed continuously either the LFD or HFD were subjected to 2 hr oral glucose tolerance tests (OGTTs). SAMP6 HFD-fed mice demonstrated the highest blood glucose levels, which peaked at 420 mg/dl at 40 min, followed by SAMP6 LFD-fed mice (300 mg/dl glucose), AKR/J HFD-fed mice (220 mg/dl), and AKR/J LFD-fed mice (200 mg/dl). **B**: The average areas under the curve (AUCs) demonstrated significantly higher blood glucose levels for SAMP6 HFD-fed compared to LFD-fed mice ($P < 0.0003$), and AKR/JHFD-fed compared to LFD-fed mice ($P < 0.03$). The AUCs also showed that blood glucose levels were significantly higher for SAMP6 HFD-fed compared to AKR/J HFD-fed ($P < 0.001$) and for SAMP6 LFD-fed compared to AKR/J LFD-fed ($P < 0.0\ 4$) mice. **C**: Plasma insulin levels were determined concurrent with the blood glucose levels. **D**: Plasma insulin levels were

significantly higher for SAMP6 compared to AKR/J HFD-fed mice ($P < 0.001$), for SAMP6 HFD-fed compared to LFD-fed mice ($P < 0.001$) and for AKR/JHFD-fed compared to LFD-fed mice ($P < 0.0\ 02$).

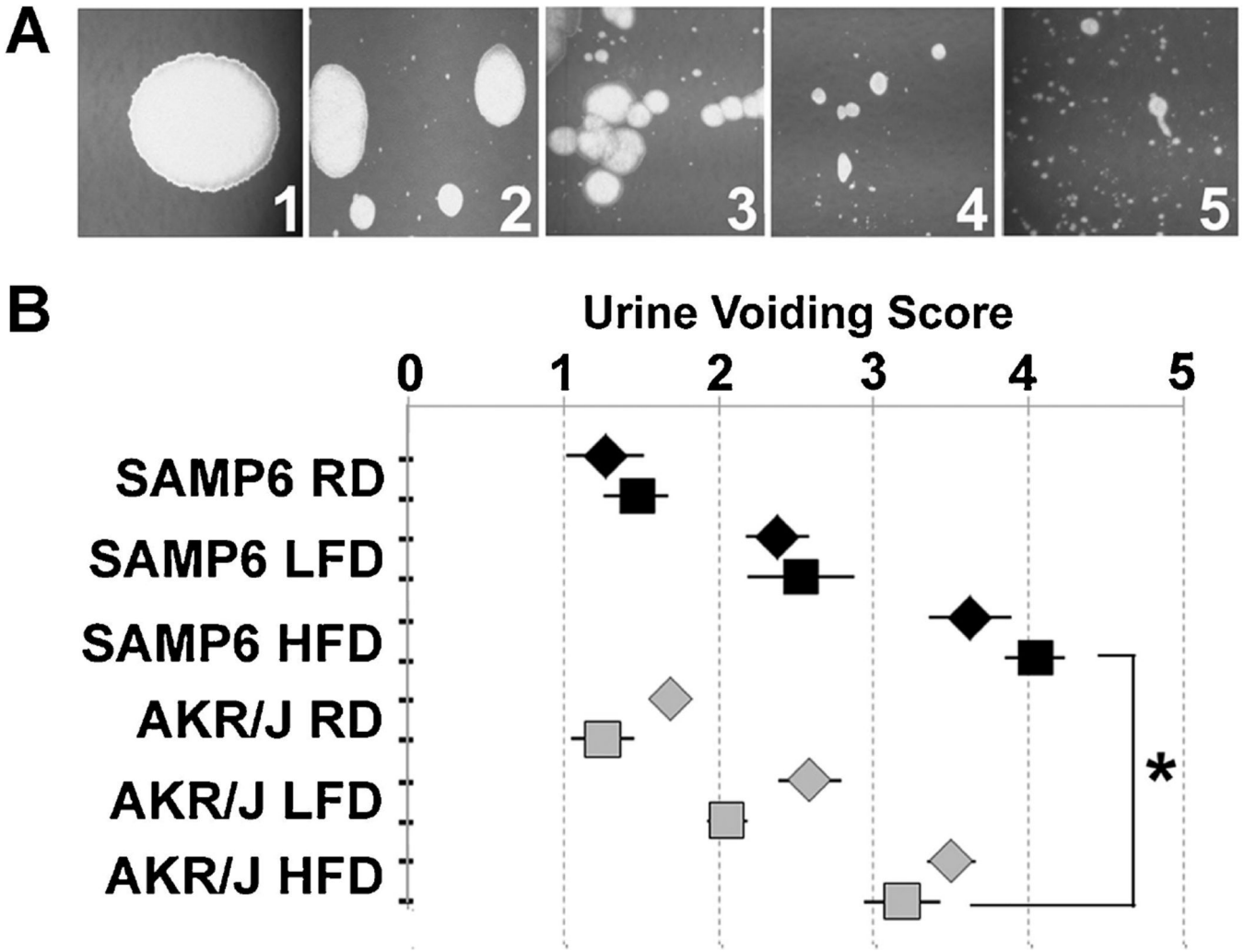

Fig. 3.

High fat diet-fed mice develop urinary voiding dysfunction. **A**: The urinary voiding pattern was graded on a scale of 1–5 depending upon the size and number of urine spots such that a score of 1 indicated the observation of single, large urine spots (no voiding dysfunction) and a score of 5 indicated the observation of many small, scattered urine spots (obstructive voiding dysfunction). **B**: Graph depicts 95% confidence intervals for urine voiding patterns for SAMP6 (black) and AKR/J (grapy) mice after 7 (diamond) or 8 (square) months of continuous feeding on RD, LFD, or HFD diets. Both SAMP6 and AKR/J mice demonstrated normal urinary voiding patterns after 7 or 8 months continuous RD-feeding. SAMP6 and AKR/J mice demonstrated similar though slightly abnormal urinary voiding patterns suggestive of mild obstruction at 7 and 8 months continuous LFD-feeding. Both SAMP6 and AKR/J mice demonstrated abnormal urinary voiding patterns suggestive of moderate obstruction for AKR/J mice and moderate/severe obstruction for SAMP6 mice at 7 and 8 months continuous HFD-feeding that was significantly worse than LFD-fed ($P < 0.008$) and RD-fed mice ($P < 0.001$). Further, SAMP6 urinary voiding dysfunction was significantly worse ($P < 0.001$) than that of AKR/J mice at both 7 and 8 months continuous HFD-feeding.

A

	SAMP6 LFD	SAMP6 HFD	AKR/J LFD	AKR/J HFD
total number	10	10	10	7
urinary retention	3	7	3	5
dermatitis	1	4	1	2

B

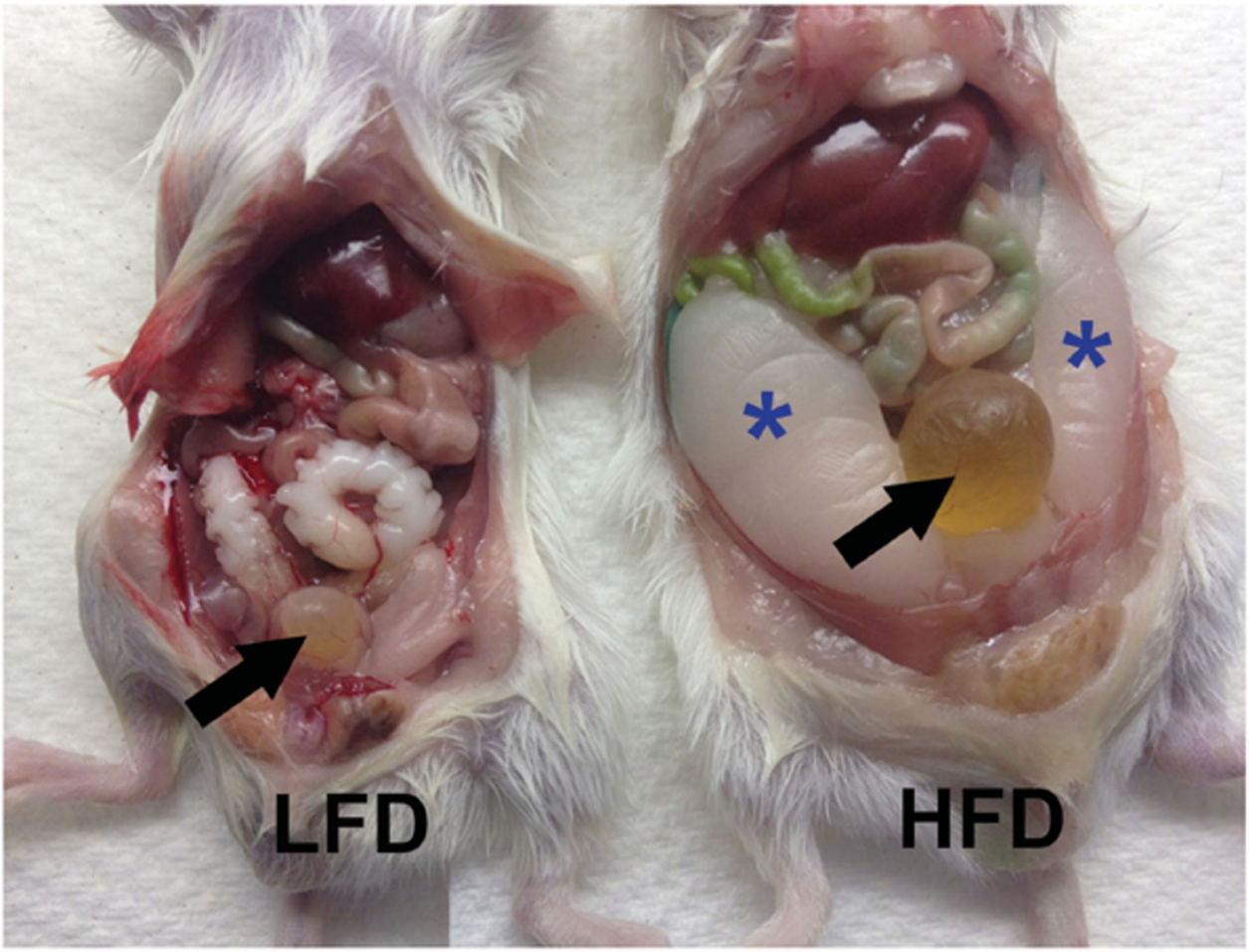

Fig. 4.

High fat diet-fed mice develop urinary retention and dermatitis. The majority of SAMP6 and AKR/J HFD-fed mice develop urinary retention (**A**) evident as inflated bladders (**B**, arrow, HFD mouse) concurrent with urinary voiding dysfunction. A smaller number of HFD-fed mice also developed chronic dermatitis (A). Epididymal fat pads are notably enlarged in SAMP6 HFD-fed mice (B, asterisks).

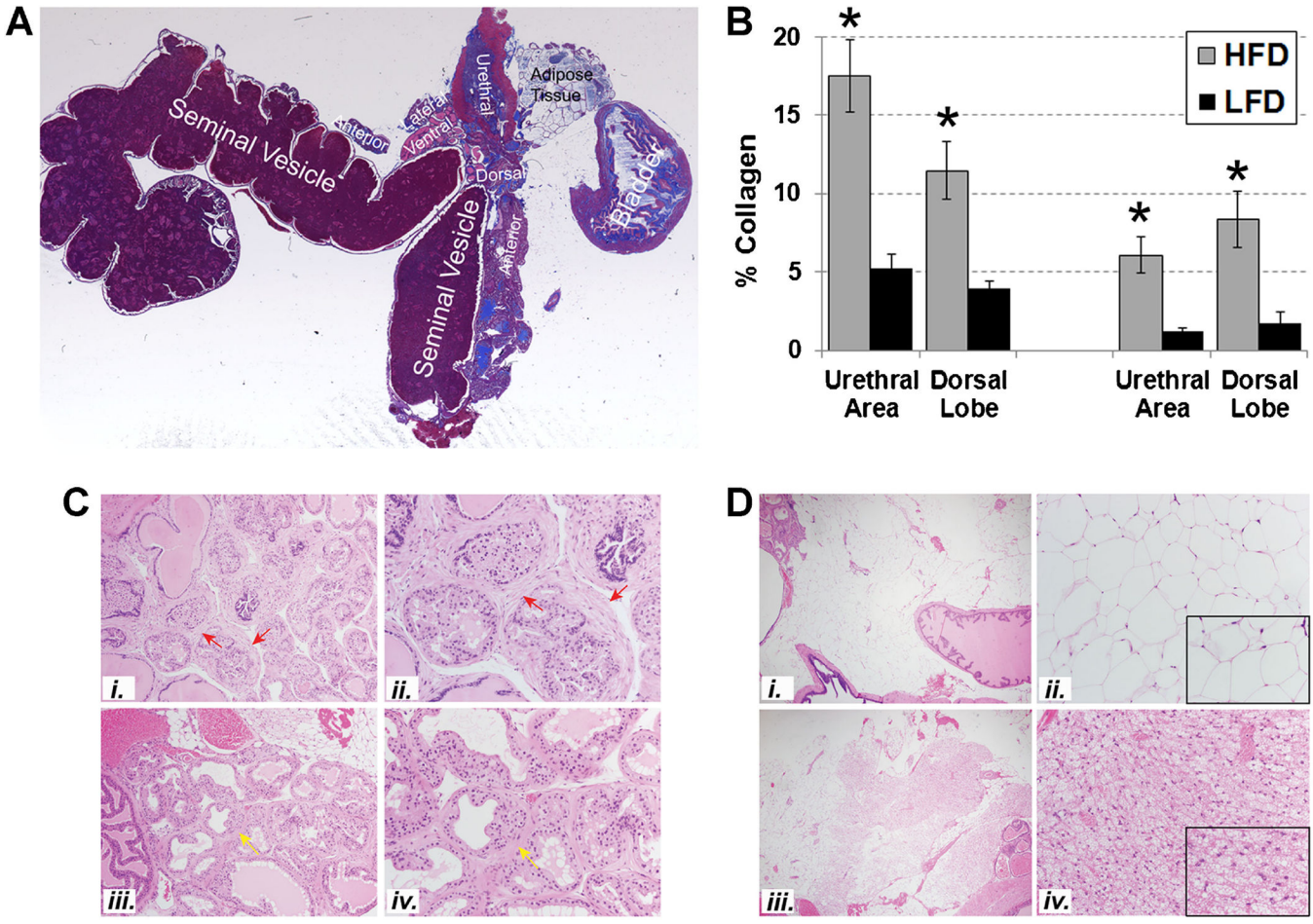

Fig. 5.

HFD-fed mice exhibit lower urinary tract fibrosis. **A**: Masson's Trichrome stained tissue sections of fixed and embedded mouse lower urinary tracts were digitally imaged and color segmented using a subprogram within MATLAB that separates and quantifies color elements from images of Masson's Trichrome stained tissues, permitting quantitation of blue-stained areas corresponding to extracellular collagen [16,23]. **B**: The percent collagen content of the prostatic dorsal lobes of SAMP6 ($P < 0.001$) and AKR/J ($P < 0.01$) HFD-fed mice demonstrated 2–4× higher collagen levels than those of LFD-fed mice ($P < 0.001$). Similarly, the urethral regions of SAMP6 ($P < 0.001$) and AKR/J ($P < 0.001$) HFD-fed mice ($P < 0.003$) demonstrated 2–4× higher collagen levels than those of LFD-fed mice. **C**: Photomicrographs (20×, i, iii; 40×, ii, iv) of serial hematoxylin/eosin stained sections to those analyzed for collagen content demonstrated peri-glandular prostatic fibrosis (red arrows) in SAMP6 HFD-fed mouse #68 (i, ii) and milder focal fibroplasia/stromal expansion (yellow arrows) in SAMP6 LFD-fed mouse #80 (iii, iv). These differences in peri-glandular fibrosis were more evident in SAMP6 HFD-fed than LFD-fed mice but did not reach, statistical significance ($P = 0.10$). **D**: Photomicrographs (4×, i, iii; 20×, ii, iv) of SAMP6 LFD-fed mice (i, ii) mice demonstrate significantly higher levels of brown adipose tissue (BAT) than white adipose tissue (WAT) compared to HFD-fed mice (iii, iv) ($P = 0.005$).

Insets in ii and iv are at 40×. Tissues are shown from SAMP6 LFD-fed mouse #68 and HFD-fed mouse #80.

Prostate. Author manuscript; available in PMC 2017 July 17.

TABLE I

Histopathological Characteristics of Murine Prostates

SAMP6 HFD	**Dorsal prostate: focal increase in cellular stroma**	**Lateral prostate: epithelial hyperplasia**	**% Brown adipose tissue (BAT)**	**AKR/J HFD**	**Dorsal prostate: focal increase in cellular stroma**	**Lateral prostate: epithelial hyperplasia**	**% Brown adipose tissue (BAT)**
62	1.5	0.0	2	84	1.0	1.0	2
63	1.5	0.0	20	85	1.0	1.0	2
64	3.0	0.0	10	87	0.0	1.0	2
65	1.0	0.0	2	88	2.0	1.0	10
68	1.5	1.0	2	89	1.5	1.0	15
70	1.0	0.0	5	90	0.0	1.0	2
71	1.0	0.0	5	91	0.0	0.0	0
66	n.i.	0.0	2	82	n.i.	0.0	30
67	n.i.	0.0	2	83	n.i.	1.0	30
69	n.i.	0.0	20	86	n.i.	1.0	2
SAMP6 LFD	Dorsal prostate: focal increase in cellular stroma	Lateral prostate: epithelial hyperplasia	% Brown adipose tissue (BAT)	AKR/J LFD	Dorsal prostate: focal increase in cellular stroma	Lateral prostate: epithelial hyperplasia	% Brown adipose tissue (BAT)
72	1.0	0.0	50	93	2.0	1.0	10
74	1.0	0.0	50	94	0.0	0.0	0
75	1.0	1.0	40	95	1.5	2.0	2
76	1.0	1.0	50	96	1.5	1.0	10
77	0.0	0.0	30	97	1.0	1.0	20
78	1.5	0.0	30	98	1.0	1.0	50
79	1.0	0.0	30	99	1.5	1.0	50
80	1.0	0.0	80				
81	1.5	0.0	10				
73	n.i.	n.i.	5				